FINITE ELEMENTS VERSUS EXPERIMENTAL FOR A CFRP STRUCTURE

R. Figueirêdo de Sá [1,2], R. Ferreira[3], N.Gonçalves[4], N. Vieira[5], J. P. Nunes [6] and F. W. J. van Hattum[7]

[1] Institute of Polymers and Composites/I3N, Minho University, 4804-533 Guimarães, Portugal
Email: sa.ricardof@gmail.com, Web Page: http://ipc.uminho.pt/
[2] PIEP - Innovation in Polymer Engineering, 4804-533 Guimarães, Portugal
Email: ricardo.sa@piep.pt, Web Page: http://www.piep.pt/
[3] PIEP - Innovation in Polymer Engineering, 4804-533 Guimarães, Portugal
Email: ricardo.ferreira@piep.pt, Web Page: http://www.piep.pt/
[4] PIEP - Innovation in Polymer Engineering, 4804-533 Guimarães, Portugal
Email: nuno.goncalves@piep.pt, Web Page: http://www.piep.pt/
[5] PIEP - Innovation in Polymer Engineering, 4804-533 Guimarães, Portugal
Email: nuno.vieira@piep.pt, Web Page: http://www.piep.pt/
[6] Institute of Polymers and Composites/I3N, Minho University, 4804-533 Guimarães, Portugal
Email: jpn@dep.uminho.pt, Web Page: http://ipc.uminho.pt/
[7] Research Centre Design and Technology, Saxion Univ. of Applied Sciences, Enschede, Netherlands
Email: f.w.j.vanhattum@saxion.nl, Web Page: https://www.saxion.edu/site/about-saxion/research-centres/design-technology/

Keywords: Optimization, FEM, CFRP, Mechanical tests, Vacuum infusion

Abstract
The work presented herein is part of a project focused on the optimization of a carbon fibre reinforced epoxy matrix (CFRP) structure. The implemented process resorts to finite elements modelling in order to evaluate the performance of the analysed structure. To validate the finite elements model at the basis of the optimization process a scale model prototype of the composite structure was built and tested under similar loading conditions. The experimental results determined were then compared with those obtained from simulations of a built numerical model depicting the experimental set up and taken into account the mechanical and geometrical properties of the composite part, the used accessories, the interface between parts and production constraints.

1. Introduction

Optimization is one of the most relevant problems related with the process of developing composite structures capable of meeting all required structural specifications for an application [1]. In fact, the many aspects that can be manipulated during the design of composite structures make them highly customizable and create new and important challenges to the need of evaluating together a great number of different variables in order to allow achieving the best final desired configuration [2]. Optimization processes based on less traditional techniques, like Metaheuristics not based on derivatives, become of great value and more important when dealing with such problems [3, 4].

In this work, finite elements were used to model, optimize and simulate the mechanical behaviour of a real composite structure, which is lightweight gantry for an industrial laser cutting equipment. A scale model prototype of the CFRP structure was built and subjected to mechanical tests to evaluate and validate the numerical modelling simulations. The mechanical and geometrical properties of the CFRP composite part, used accessories, interface between parts and production constraints were taken into account in the numerical model used in simulations. Good agreement has been found between results

experimentally determined on the loaded manufactured CFRP structure to those obtained from the numerical model simulations.

2. Material and Methods

2.1. Part Geometry

The manufactured composite prototype used in the tests was constituted by 8 different components, all of them produced by vacuum infusion. Two of them are 700 mm long and, when assembled together, form a square tube with a section of 100 mm of external dimension and with walls approximately 1.8 mm thick. These two parts, represented in blue in Figure 1, were manufactured with tabs (shown in red in Figure 1) to allow applying the adhesives used to tightly assemble both together. This tube is reinforced by 6 ribs glued to its internal surface (represented in yellow). These ribs allow increasing the overall stiffness of the structure.

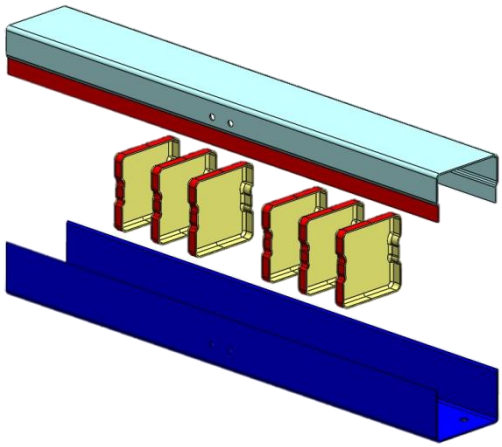

Figure 1. Overview of the designed prototype.

2.2. Materials

Plain weave carbon fibre fabrics from MITSUBISHI RAYON CO, PYROFIL™ TR30S 3K with a density of 195 g/m2, were used to manufacture the composite tested prototype employing the laminate layer stacking sequence described in Table 1.

Table 1. Layer stacking sequence.

Layer	*Orientation*
9 *8* *7*	*±45º*
6 *5* *4*	*0 – 90º*
3 *2* *1*	*±45º*

An epoxy resin was used as matrix by mixing, on a mass ratio of 100:30, the EPIKOTE™ Resin 04908 with the EPIKURE™ hardener 04908 from HEXION™. All different components were produced by vacuum infusion resorting to moulds produced from tooling block and coated with a Polyurethane paint. The adhesive EPX™ DP490 from 3M was used to assemble. A thickness of 0.8 mm was established as goal to apply the adhesive. Such dimension was accounted during design and all production stages of the composite parts, as well as in the assembling process.

Standard samples were produced by vacuum infusion using the same carbon fibres and epoxy matrix to be tested and allow characterizing the used laminate layers and obtain the input properties for the finite elements analysis. Tensile tests were performed on these composite layer samples reinforced with plain weaves 0/90° oriented carbon fibres. They were conducted according to ASTM D3039/D3039M-08 - "Test Method for Tensile Properties of Polymer Matrix Composite Materials" and allowed to obtain Young modulus, ultimate stress and Poisson´s ratio of the laminate. Table 2 presents the results determined from the tests made on 8 samples at room temperature. The samples were produced from the same fibres and using the same matrix.

Table 2. Laminate tensile properties

Property	*Value (average)*	*Standard Deviation*
Ultimate stress (MPa)	*781.05*	*23.41*
Young Modulus (GPa)	*59.81*	*0.98*
Poisson Coefficient	*0.05*	*0.01*

The behaviour of the adhesive was also characterized using single lap joint samples produced by binding two composite laminates manufactured using the previously listed materials. The tests were performed accordingly to the standard ASTM D 3165-00 – "Test Method for Strength Properties of Adhesives in Shear by Tension Loading of Single-Lap-Joint Laminated Assemblies". Five samples were tested and an average value of 18.06 ± 1.5 MPa was obtained as maximum shear stress. The tests also allowed evaluating if any damage was inflicted to the adhesive layer and if it will be able to withstand the shear loads to which the final composite prototype is expected to be subjected.

2.3. Loading scenario

The produced composite prototype was subjected to an off-centred load of 5 kN applied perpendicular to its axis at the midpoint lengthwise (see Figure 2). The load was applied distributed on 50 mm x 50 mm area of a L-shaped steel profile (in red in Figure 2) glued and also tightly attached to the face of the part by 4xM4 screws. In order to minimize deformation, the selected steel bearing profile had a thickness of 10 mm. The prototype was perfectly restrained at its both extremities, being tightly connected to the steel I profile beams of the testing equipment through 90 mm x 140 mm areas. The application of the 5 kN load will result in the development of bending and torsion efforts on the composite prototype.

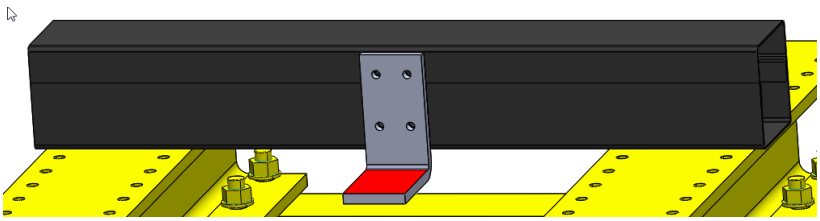

Figure 2. Prototype mounted on I profile beams with highlighted load application area.

2.4. Experimental Testing

The testing was performed having the part mounted to two I section steel beams with four M10 screws on each fixation surface. To ensure load distribution a glass fibre pultruded plate was used to compress the part's walls (Figure 3 - 1). The 5 kN load was then applied using a hydraulic actuator (maximum load of 20 kN) (Figure 3 - 2) with a constant 1.5 mm/min displacement speed. The L steel profile transmits the applied load and ensures that the loading application area remains constant (at least for the small displacement verified), as well as the direction of the applied load. Three Linear Variable Differential Transformers (LVDTs) were used to measure displacement at different points considered as critical. The LVDT a) was placed in the part's surface opposed to the loading location. LVDT b) was located at a distance of 150 mm from LVDT a. LVDT c) was placed touching the lower surface on the same plane but perpendicular to the LVDT a) axis. Figure 3 - 3 is a planar rectangular rosette used to measure the local strain. Values were recorded for the actuator's displacement and force, the three LVDTs displacements and the strains for the three gauges of the rosette.

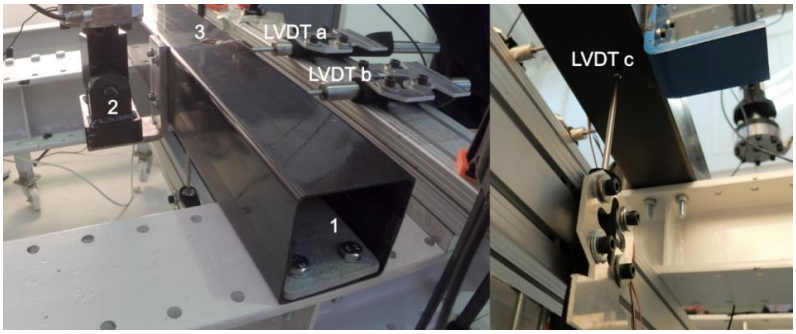

Figure 3. Experimental set-up overview.

2.5. Numerical Simulation

The numerical simulations were performed using Abaqus/CAE 6.11-1. The geometry depicts the produced prototype composed by the same number of composite parts used in the experimental tests. All composite parts refereed as 1 in Figure 4, as well as the I section beams and actuator (2 and 3 in Fig. 4), were modelled as shell elements. While components 1 were attributed mechanical properties according to the ones determined experimentally, the rest of the shell elements, 2 and 3, were considered totally rigid, meaning they will suffer no deformations. The load bearing element 4 was modelled as a 3D solid element. The offset between parts to ensure an adequate adhesive thickness was not considered (which results in the overlapping between them in the tabs).

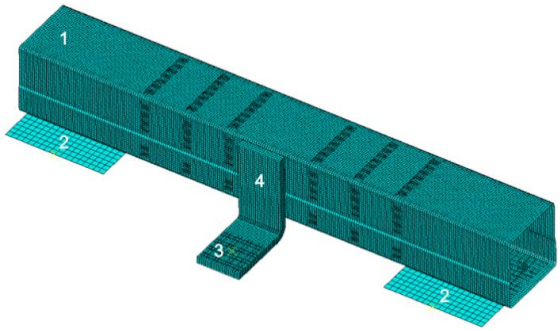

Figure 4. Overview of meshed Finite elements set-up.

The values of the CFRP layers determined experimentally were used for modelling. A layup that follows the one specified in Table 1 was created and applied to the components. The mechanical properties listed in the manufacturer datasheet were used to model the steel components presented in the set-up (a Young Modulus of 212 GPa and a Poisson coefficient of 0.3). An important assumption considered in the model was that low tensions and deformation were expected. This implies that none of the materials reaches its ultimate stress or strain and, in the case of the steel, it would not suffer any plastic deformation. Following this principle, only the elastic part of the materials' behaviour was considered.

The interactions between parts were modelled using a tie constraint. This means no separation is allowed between them. Underlying this formulation is the assumption that the adhesive always withstands all the loads it is subjected to and the shear stress was then evaluated in the outer layers of the bounded surfaces. If the shear strain values will be near the ones determined experimentally for the maximum adhesive shear loading, than a more detailed model of the adhesives behaviour should be implemented.

While all parts were considered being perfectly restrained in screwing attached areas and compressed by the glass fibre pultruded plate , surrounding zones could slide over the rigid supports (I steel beams from the experimental set-up), as they may become in contact upon deformation.

The actuator is also considered to be completely tied to the load bearing element. The load consists of a concentrated force applied through the centre of the actuator rigid surface. This results in a distributed force transmitted to the loaded bearing element, which is applied along the same axis as happen in the experimental set-up.

3. Results and Discussion

3.1. Numeric Results

The simulations show the composite structure, in general, subjected to low levels of stresses (Figure 5) and that the highest stresses occurred at points located on its interfacing surfaces, with either the support structure or the load bearing element.

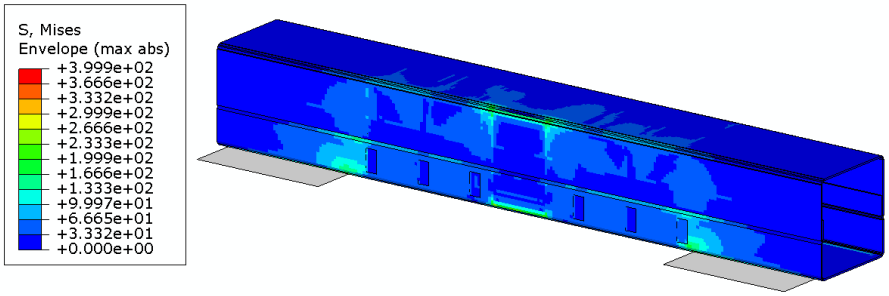

Figure 5. Stress (Misses) for the composite elements.

The maximum stress values around 400 MPa obtained in numerical simulations are much lower than the 781.05 MPa ultimate stresses experimentally determined for the material.
As Figure 6 shows, the adhesive is also subjected to shear stresses quite bellow the one determined experimentally as its shear strength (≈18.1 MPa).

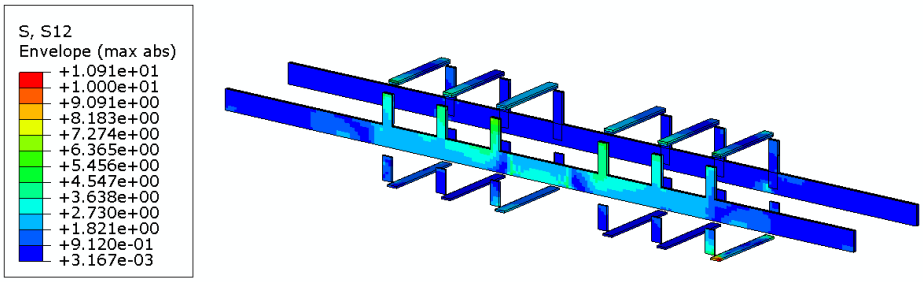

Figure 6. Shear stress in the adhesive interfaces.

3.2. Numerical and experimental results comparison

As previously mentioned, the experimental tests were monitored by logging the applied force and displacement of the actuator, the values of displacement using 3 different LVDTs and a planar rectangular rosette. Data for comparing with these control mechanisms was also extracted from the numerical simulation's results.

The displacement data was obtained by determining the intersection of a straight line defined according to the position of the LVDTs with the surface of the part. Figure 7 compares the experimental displacements obtained from LVDTs 1 to 3 and those determined numerically in the same location in function of the applied load.

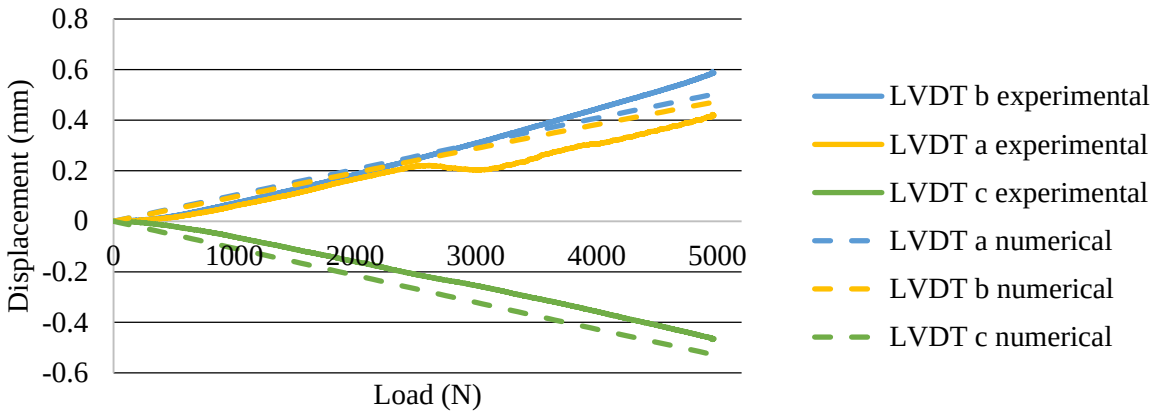

Figure 7. Compairison of local displacement in experimental and numerical testing.

It is visible that the values determined numerically and experimentally are quite similar. It is also shown that the variations of the numerical displacements are directly proportional to the load, while the experimental tests have a less linear behaviour. This allows concluding that the approximation presented by the numerical model is valid and quite representative of the overall behaviour.

Figure 8 presents the comparison between the actuator displacements as function of the applied force determined both in the numerical and experimental tests.

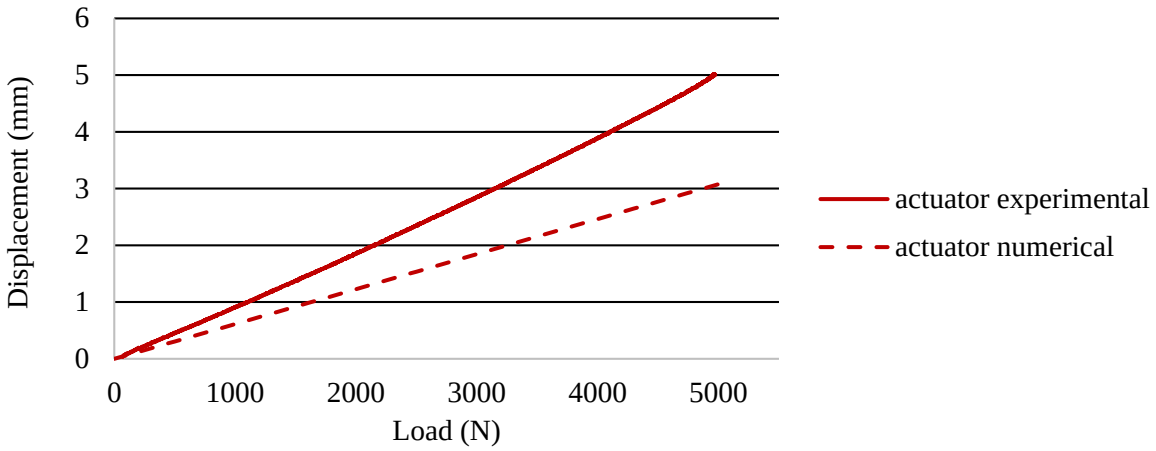

Figure 8. Comparison of local displacement in experimental and numerical testing.

The difference seen between the theoretical simulations and experimental data may be justified by the following reasons: i) the difference between the real a theoretical properties used in the numerical simulations for the load bearing, ii) the relative movement that occurs between the composite part and the I steel supporting beams, iii) Deformations that might occur in the testing rig and it was considered rigid in the numerical model.

Regarding the outputs from the planar rosette, it is necessary to ensure that both experimental and numerical obtained values are consider in the same direction, meaning that both outputs must have the axis of the rosette in the same direction. After determining the strains in each of the three directions of the rosettes (A, B and C), the maximum (Eq. 1) and minimum strains (Eq. 2), as well as the angle of main strains with the A gage (Eq. 3) can be calculated using the following known strain-transformation relationship [5].

$$\varepsilon_{max} = \frac{\varepsilon_A + \varepsilon_C}{2} + \frac{1}{\sqrt{2}}\sqrt{(\varepsilon_A - \varepsilon_B)^2 + (\varepsilon_B - \varepsilon_C)^2} \quad (1)$$

$$\varepsilon_{min} = \frac{\varepsilon_A + \varepsilon_C}{2} - \frac{1}{\sqrt{2}}\sqrt{(\varepsilon_A - \varepsilon_B)^2 + (\varepsilon_B - \varepsilon_C)^2} \quad (2)$$

$$\varphi = \frac{1}{2} tan^{-1}\left(\frac{\varepsilon_A - 2\varepsilon_B + \varepsilon_C}{\varepsilon_A - \varepsilon_C}\right) \quad (3)$$

Figure 9 shows the minimum and maximum strains (principal strains) observed both from the experimental and numeric tests, as well as their orientation with respect to the rosette A axis.

It is visible that the direction of the principal strains is coincident. However the strains presented slight variations. An analysis of the strain state at each considered location shows that the results obtained experimentally presented slight higher strains than the numerical simulations. Despite these small differences, it can be concluded that a quite good agreement was obtained between the theoretical and experimental results.

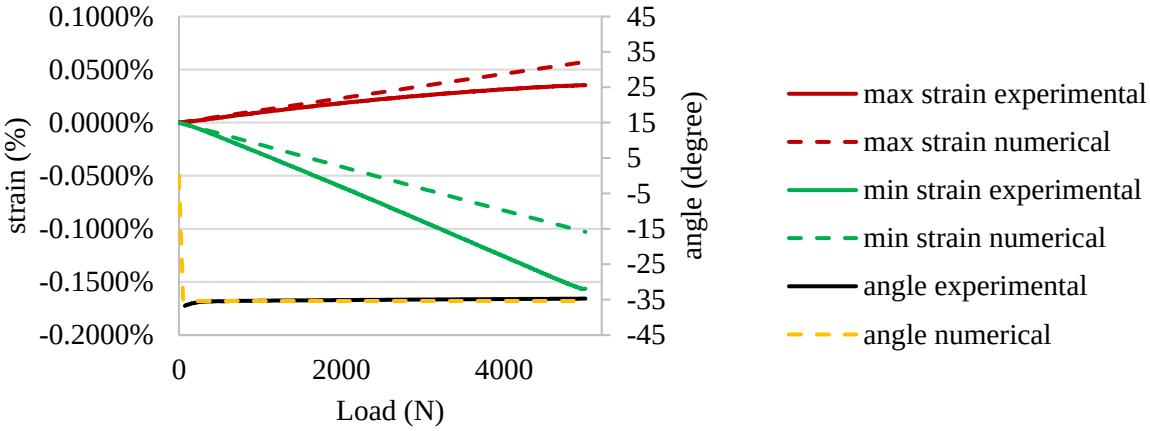

Figure 9. Comparison of principal strains and their orientation in experimental and numerical testing.

4. Conclusions

A study to validate the finite elements model by direct comparison to an experimental test was performed. The experimental results, determined on a CFRP part produced by vacuum infusion, were monitored using three LVDT sensors and a rectangular rosette, all of which located in points considered of strategic significance. The numerical results show that the part is able to sustain the loads without reaching the ultimate stress or the ultimate shear stress of the adhesives. The comparison between experimental and numerical results shows that the finite element model renders accurate results. Some deformation of non-composite components or testing equipment should be accessed and included in the finite element analysis for better accuracy.

Acknowledgments

Authors acknowledge the support given by the Portuguese Foundation for Science and Technology under project UID/CTM/50025/2013 and scholarship SFRH / BD / 51106 / 2010. The authors also acknowledge the support and means provided by PIEP – Innovation in Polymer Engineering.

References

[1] Schmit, L.A. and B. Farshi, Optimum laminate design for strength and stiffness. International Journal for Numerical Methods in Engineering, 1973. 7(4): p. 519-536.
[2] Paluch, B., M. Grédiac, and A. Faye, Combining a finite element programme and a genetic algorithm to optimize composite structures with variable thickness. Composite Structures, 2008. 83(3): p. 284-294.
[3] Conn, A.R., K. Scheinberg, and L.N. Vicente, Introduction to Derivative-Free Optimization. MPS-SIAM Book Series on Optimization, ed. SIAM. 2009.
[4] Oliveira Junior, H.A., et al., Stochastic Global Optimization and Its Applications with Fuzzy Adaptive Simulated Annealing. 2012: Springer Heidelberg.
[5] TN-515 - Strain Gage Rosettes: Selection, Application and Data Reduction. 2014, Micro Measurements.